

## **DELTA FORMATION IN RESERVOIRS OF RUN-OF-RIVER HYDROPOWER PLANTS IN GRAVEL BED RIVERS – EXPERIMENTAL STUDIES WITH NONUNIFORM SEDIMENTS**

CHRISTINE SINDELAR<sup>(1)</sup>, THOMAS GOLD<sup>(1)</sup>, KEVIN REITERER<sup>(1)</sup>, JOHANNES SCHOBESBERGER<sup>(1)</sup>,  
PETR LICHTNEGER<sup>(1)</sup>, CHRISTOPH HAUER<sup>(1)</sup> & HELMUT HABERSACK<sup>(1)</sup>

<sup>(1)</sup> CD-Laboratory for Sediment research and management, Institute for Hydraulic Engineering and River Research, Department for Water – Atmosphere – Environment, University of Natural Resources and Life Sciences, Vienna, Austria  
christine.sindelar@boku.ac.at; thomas.gold@students.boku.ac.at; kevin.reiterer@students.boku.ac.at;  
johannes.schobesberger@boku.ac.at; petr.lichtneger@boku.ac.at; christoph.hauer@boku.ac.at; helmut.habersack@boku.ac.at;

### **ABSTRACT**

This study concerns scaled physical model tests of the delta formation process at the head of a run-of-river hydropower plant (RoR). It forms part of a larger research project to provide a scientific base for RoR sediment management strategies in medium-sized gravel bed rivers. The physical model consisted of an idealized river having a width of 20 m, a mean slope of 0.005, a mean flow rate of 22 m<sup>3</sup>/s and a 1-year flood flow of 105 m<sup>3</sup>/s. The model scale was 1:20. For the experiments five different grain sizes were used covering a range of 14 to 120 mm. Sediment feeding rates for each grain size were calculated using the surface-based approach of Wilcock & Crowe (2003) which was calibrated in preliminary tests in a straight channel. Experiments were carried out under live-bed conditions at a flow rate which corresponds to 70% of the 1-year flood. This discharge is able to mobilize all sediment fractions and is yet low enough to not evoke reservoir drawdown. It is therefore well suited to study delta formation. Two sets of test runs were performed: (i) normal flow conditions to provide a reference case which is undisturbed of any backwater effects and (ii) delta formation at the head of the reservoir at turbine operation (i.e. at operation level). The experiments revealed that even at the head of the reservoir which is least influenced by the backwater effect of the RoR plant sediment transport practically ceases for sediment fractions > 14 mm at 1:1 scale. The whole sediment load coming from the undisturbed upstream section accumulates at the head of the reservoir accompanied by a substantial rise in water levels.

**Keywords:** physical model test, heterogeneous grain size distribution, delta formation, run-of-river hydropower plant

### **1 INTRODUCTION**

In the recent decades, human activities and climate change-related effects have disturbed the natural sediment dynamics of the rivers and streams worldwide. Direct results of such disturbances may include sediment deficit in river reaches, which could cause bed degradation, lowering of ground water levels, wetland drying, attenuation of water-land connectivity, and endangering the structural safety of infrastructures (Sindelar et al., 2019). Sediment deficit also promotes coastal erosion at the mouth of large rivers (e.g. Danube, Mississippi). On the other hand, surplus of sediments could lead to reservoir sedimentation. Today, more storage volume of reservoirs is lost than is gained by the construction of new reservoirs, leading to a situation that is neither sustainable nor economically justifiable (Annandale et al., 2018). Understanding sediment processes in rivers is essential for developing efficient sediment management strategies to tackle the sediment deficit and surplus problem in riverine systems (Best, 2019; Habersack et al., 2013; Hauer et al., 2018). Riverine systems need to preserve connectivity in order to fulfill ecosystem processes and biodiversity. Recently, the connectivity status of rivers was examined revealing that very few large rivers around the world provide long free-flowing sections, most of which are located in sparsely populated areas (Grill et al., 2019). The connectivity status was assessed based on (1) river fragmentation (longitudinal); (2) flow regulation (lateral and temporal); (3) sediment trapping (longitudinal, lateral and vertical); (4) water consumption (lateral, vertical and temporal); and (5) infrastructure development in riparian areas and floodplains (lateral and longitudinal). Dams and reservoirs were identified as major contributors to the loss of river connectivity (Grill et al., 2019). According to the European Water Framework Directive (WFD), a river reach achieves a “very good ecological status” if the continuity is not disturbed by anthropogenic activities and allows undisturbed migration of aquatic organisms and sediment transport. To reach a “good ecological status”, sediment continuity is implicitly included based on biological requirements (Habersack et al., 2014), however, not directly formulated as a target. Thus, sediment continuum and dynamics were frequently neglected as a backbone to achieve a sustainable “good ecological status” (compare to Hauer, 2015). In many Alpine rivers reaches, however, the

sediment continuity is disturbed by run-of-river hydropower plants (RoR) which significantly alter river morphodynamics. On the other hand, hydropower accounts for approximately 60% of the generated electricity in Austria thus contributing to the fulfillment of the objectives of the Renewable Energy Directive (RED) of the European Union. In Austria 87% of the RoR plants are located in small and medium-sized rivers and have an installed capacity of <1 MW each (Wagner et al., 2015). In order to develop sustainable sediment management strategies for RoR plants in gravel bed rivers it is import to understand the underlying physical processes, especially for nonuniform sediment mixtures. Such natural nonuniform sediment sorting was frequently neglected in terms of physical modelling of reservoir sedimentation processes up to now. As a river reach enters the head of a RoR reservoir backwater effects greatly influence the morphodynamics. A delta forms at the head of the reservoir. Longitudinal, lateral and vertical sediment sorting occurs as the river approaches the dam. Only the finest fractions of the sediments reach the dam. Although these principal processes are well known, modelling sediment transport of heterogeneous sediments, specifically in nonuniform flow, remains a challenge: mathematically, experimentally and numerically.

Thus, the experimental work in this paper aims at describing delta formation at a RoR plant during turbine condition (i.e. at operation level) with nonuniform sediments. The experiment includes a supportive analysis with the surface-based transport model of Wilcock & Crowe (2003).

## 2 EXPERIMENTAL SETUP AND METHODS

### 2.1 Representative medium sized gravel bed river

To study delta formation in a representative medium-sized gravel bed river experimentally, hydrological and sedimentological characteristics were taken from the Mürz river in Styria, Austria. The Mürz river is 83 km long. Its basin which is located north of the Central Alps covers an area of 1,500 km<sup>2</sup>. The Mürz belongs to the Danube river system. The source (confluence of Stille Mürz and Kalte Mürz) is at 840 m a.s.l.. The Mürz flows into Mur river in Bruck an der Mur at 470 m a.s.l.. Altogether, 23 RoR hydro power plants and 6 diversion plants are located along the Mürz. Their hydraulic heads range from 3 to 10 m (Sindelar et al., 2017). The mean bed slope, mean river width as well as hydrological and sedimentological conditions of the Mürz river at gauging station Kapfenberg-Diömlach, 2.8 km upstream of the mouth, are summarized in Table 1. The bed material consists of gravel and sand with maximum grain sizes > 0.1 m, the  $d_m$  is 0.06 m.

**Table 1.** Mean bed slope, mean river width, hydrological and sedimentological conditions of the Mürz river at gauging station Kapfenberg-Diömlach, 2.8 km upstream of the mouth.

Catchment area (km <sup>2</sup> )	Mean flow MQ (m <sup>3</sup> /s)	design flow RoR (m <sup>3</sup> /s)	1-year flood (m <sup>3</sup> /s)	10-year flood(m <sup>3</sup> /s)	Mean bed slope (-)	Mean river width (m)	$d_m$ (m)
1364.5	22	35	105	219	0.005	20	0.06

### 2.2 Experimental Setup

A physical model at a length scale of 1:20 was constructed in the Hydraulics Laboratory of the University of Natural Resources and Life Sciences, Vienna to study the delta formation with nonuniform sediments at the head of a reservoir. The physical model consisted of an idealized straight river having a width of 20 m and a mean slope of 0.005. The physical model was 15 m long and covered three sections: (i) inlet basin with flow straighteners, (ii) experimental section and (iii) outlet section with a sand trap and a flap gate to control the water levels in the model where necessary (Sindelar et al., 2017). The experimental section was 10 m long (Figure 1).

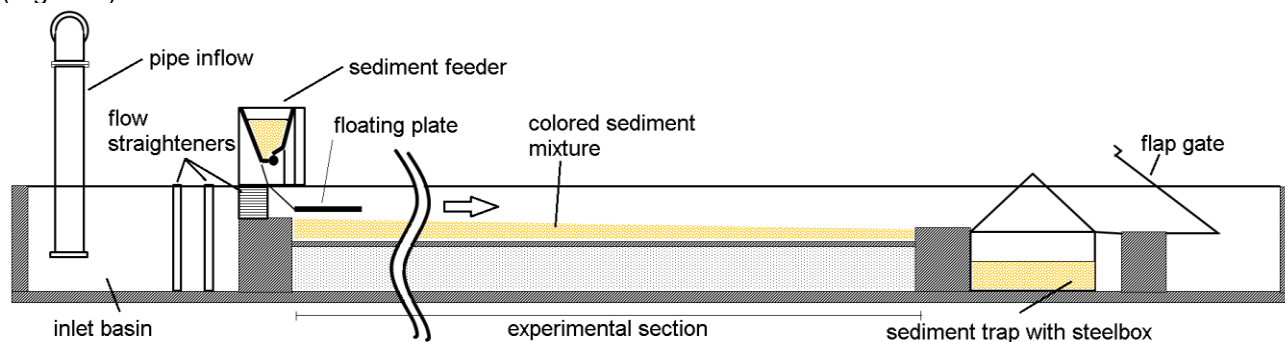


**Figure 1.** Experimental setup, longitudinal cut.

The side walls of the model are 1.33 m apart. On either side of the model square pipes (30 x 30 mm) were mounted on the side walls which were height and slope adjustable by means of slot holes. For the present experiments the width of the model was restricted to 1 m. The water supply came from the central water circulation system of the laboratory. The concrete bottom of the physical model was filled up with mobile sediments. At the downstream end of the experimental section a 0.5 m long sloping plastic panel was placed to avoid sediment entrainment of the experimental section into the sand trap. To adjust the desired bed slope the longitudinal pipes were leveled accordingly. Then a wooden vertical panel was moved along the slope-adjusted pipes manually.

### 2.3 Sediment mixture

A sediment mixture of five different grain sizes ranging from 0.7 – 6 mm was used in the experiments to be able to study sorting processes which play a dominant role in reservoir siltation and delta formation. Each grain fraction had a different color (Table 2). This has two main advantages: first, sorting processes are easily visible by eye and second, by applying image processing methods the grain size distribution of the bed surface can be determined automatically. The initial grain size distribution of the bed surface was chosen to resemble the grain size distribution of the Mürz river. For simplicity grain sizes < 0.7 mm were not considered to avoid cohesive forces between the sediments.

**Table 2.** Sediment mixture of five different fractions: grain size, color and initial mass fraction

Fraction No.	Grain size (mm)	Grain size 1:1 (mm)	Color	Initial mass fraction (%)
1	0.7 – 1.2	14 – 24	Yellow	15
2	1.2 – 2.0	24 – 40	Red	15
3	2.0 – 3.0	40 – 60	Green	20
4	3.0 – 4.0	60 – 80	Black	25
5	4.0 – 6.0	80 – 120	White	25

### 2.4 Instrumentation

The discharge was adjusted with frequency controlled pumps and was measured using a electromagnetic flow meter. Along the 10 m long experimental section 11 stations  $X_i$  were defined where the water levels were measured in two lateral positions  $Y = \pm 0.25$  m ( $Y = 0$  representing the channel axis) with a point gauge at the end of each test run. A novel, in-house developed sediment feeder - having an accuracy of  $\pm 5\%$  - supplied the physical model with the pre-defined sediment rates. The bed levels were determined by means of photogrammetry. The laboratory is equipped with a three-axes positioning system which was used to take pictures of the model at predefined positions (X,Y,Z). A total of 45 pictures of the experimental section were taken with an overlap of 80% using a Nikon D7100 camera (lens: AF NIKKOR 20mm, F/2.8D; resolution: 6000 x 4000 pixels). Each picture featured several ground control points (GCP) on both side walls of the physical model. Each GCP was equipped with a unique circle bar code and its coordinates were known at an accuracy of  $\pm 0.1$  mm. The software Agisoft Metashape 1.5.2 automatically detected the GCPs on the pictures and calculated an orthophoto and a digital elevation model (DEM) of the bed levels. In addition to the 45 pictures 60 more images of the experimental section were taken each covering a smaller section, thereby increasing the pixels per  $\text{mm}^2$ . This way the pixel size was  $0.08 \times 0.08 \text{ mm}^2$ . As a result, even the smallest grains with a diameter of 0.7 mm were represented on the image by several pixels. These high-resolution images were used to calculate the grain size distribution by assigning each pixel of the deskewed and aligned image to one of five color classes. This was done by using a maximum likelihood classification including predetermined signature classes in ArcMap Version 10.5. Figure 2 illustrates a  $0.12 \times 0.12 \text{ m}^2$  section of an image (a.), the processed image where each pixel belongs to exactly one color class (b.) and the resulting grain size distribution (c.).

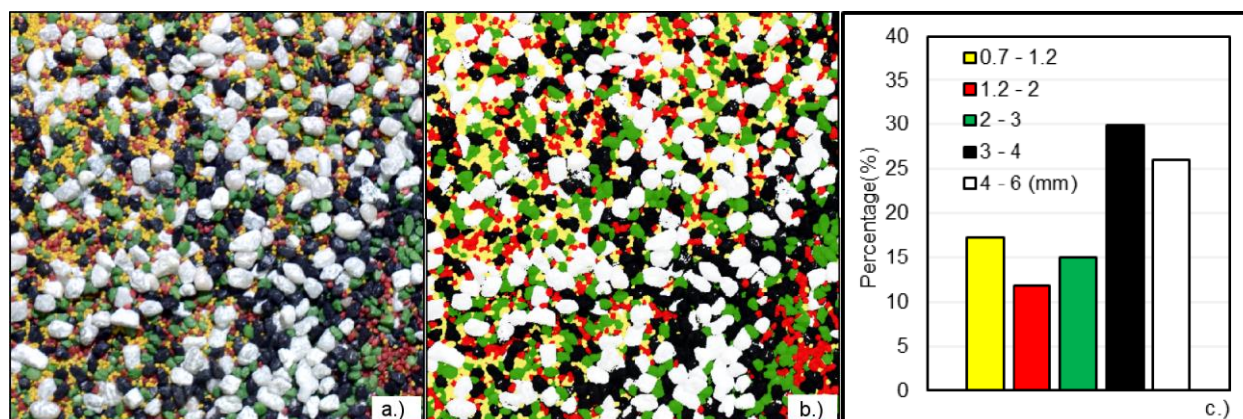


**Figure 2.** (a) aligned image of the sediment mixture covering an area of 0.12x 0.12 m<sup>2</sup> (b) processed image assigning each pixel to one of five color classes (c) resulting grain size distribution.

## 2.5 Test conditions and procedure

Two different sets of experiments were carried out: (1) reference test runs without backwater effect and (2) a delta formation test runs, respectively. In both sets the flow rate was 70% of a 1-year flood,  $Q = 0.7 \times Q_{1\text{-year}}$ . At this discharge all fractions of the sediment mixture were transported. Assuming that the reservoir of a RoR plant is not drawn down, this flow rate represents a good test case to study delta formation. First, reference test runs starting from a plane bed at a slope of 0.005 were carried out to determine the dynamic equilibrium slope of the bed during sediment transport, i.e. under live-bed conditions. The sediment transport rate was pre-calculated using the bimodal sediment mixture model of Wilcock and Crowe (2003) and was verified in preliminary tests. The water surface in the model was subject to the roughness of the bed and the transported sediments and was not controlled by the flap gate. The initial test conditions are summarized in Table 3, where  $U$  = mean velocity,  $g$  = gravitational acceleration,  $H$  = water depth,  $\nu$  = kinematic viscosity,  $\rho_w$  = density of water,  $\rho_s = 2650 \text{ kg/m}^3$  = density of sediments,  $\tau$  = shear stress,  $u_\tau$  = shear velocity and  $D_m$  = mean grain diameter,  $Fr$  = Froude number,  $Re$  = Reynolds number,  $Fr^*$  = dimensionless shields stress,  $Re^*$  = particle Reynolds number.

**Table 3.** Initial test conditions in the scaled model

Flow rate (l/s)	Sediment rate (kg/sm)	bed slope (-)	$Fr = U / \sqrt{gH}$	$Re = UH/\nu$	$Fr^* = \tau / [(\rho_s - \rho_w)gD_m]$	$Re^* = u_\tau D_m / \nu$
41.1	0.0122	0.005	0.83	41,000	0.064	167

Second, the delta formation test started from the final equilibrium bed levels from the reference case, backwater conditions were adjusted in the middle of the experimental section as follows: From the reference tests the equilibrium normal depth  $H_{eq} = 0.063 \text{ m}$  was known. The backwater curve of a reservoir approaches the normal depth upstream asymptotically. The head of a reservoir is therefore often defined as the longitudinal station  $X_{head}$  where the water depth  $H = 1.01 \cdot H_{eq}$ . In the experiments  $X_{head} = 4.4 \text{ m}$  (i.e. the middle of the experimental section) was chosen as the location of the head of the reservoir to allow delta evolution in the up- and downstream direction, respectively. A point gauge was positioned at the elevation where  $H = 1.01 \cdot H_{eq}$ . Then the discharge was set and the desired water depth was adjusted by means of the downstream flap gate. This was a very time-consuming and sensitive procedure. For minimal changes in the top edge of the flap gate it took 10-15 minutes until the water depth was adjusted.

The procedure for the reference case as well as for the delta formation case was similar. Each set of experiments consisted of eight tests lasting for one hour each. Then model was filled with water from the downstream end at a very low flow rate to avoid bed level changes during the filling process. The flap gate was used to achieve high water surface elevations. The sediment load for one hour was added to the sediment feeder. Then the discharge was adjusted, the flap gate was lowered to a position where it did not influence the water levels in the model any longer and the sediment feeder was started. During the final 15 minutes of each test run the water levels were measured with a point gauge at two lateral positions ( $Y = \pm 0.25 \text{ m}$ ) for 11 longitudinal stations. At the end of a test run the water levels were raised with the flap gate. Sediments that were entrained during the experiment were collected in a steel box covering the whole area of the sand trap. The weight of the entrained sediments under water was determined using a crane weigher. Later the entrained sediments were dried and a sieve analysis was done. When an even number of test hours had passed (2, 4, 6 and 8 hours) the water was slowly drained out of the model and the bed levels were

photographed twice: (i) to obtain the DEM from photogrammetry and (ii) to get the grain size distribution of the bed surface by means of image processing (section 2.4).

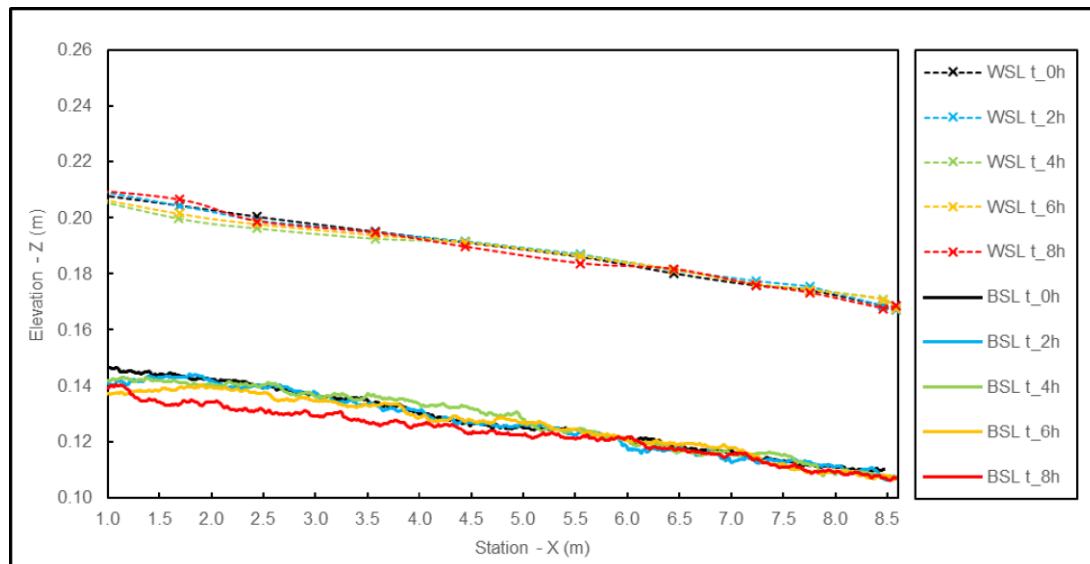
### 3 EXPERIMENTAL RESULTS

#### 3.1 Reference test runs

The reference test runs were carried out to determine the dynamic equilibrium bed slope of the sediment mixture under live-bed conditions. Flow rate, grain size distribution of the fed sediments as well as the feeding rate were independent variables (Table 3). Eight test runs were carried out. In Table 4 the mean bed and water surface slopes, the location of the thalweg as well as the ratio of fed vs entrained sediment load are summarized after 0, 2, 4, 6 and 8 hours. The mean bed slope was determined as follows: at each station X the bed elevation was calculated as the mean value of the bed elevations at  $Y = -0.25\text{m}$ ,  $Y = 0\text{m}$  and  $Y = 0.25\text{m}$ . A linear fit of the mean bed levels between  $X = 2\text{m}$  and  $X = 7\text{m}$  was used to determine the mean bed slope. The calculation of the water surface slope was analogous except that there were only two water surface measurements for each station X.

**Table 4.** Mean bed and water surface slopes, thalweg location and ratio of fed vs entrained sediment load for the reference case

Test hour (h)	Bed slope	Water surface slope	Thalweg location	Ratio of fed vs entrained sediment load
0	0.0054	0.0052	Plane bed	-
2	0.0056	0.0052	Upstream-right to downstream-middle	0.85
4	0.0055	0.0046	Upstream-left to downstream-middle	0.94
6	0.0044	0.0048	Upstream-middle to downstream-left	1.10
8	0.0035	0.0044	Upstream-middle to downstream-right	1.09
mean	0.0049	0.0048	Middle	1.00



In Figure 3 the mean bed and water surface evolution is illustrated for the test runs 0, 2, 4, 6 and 8 hours.

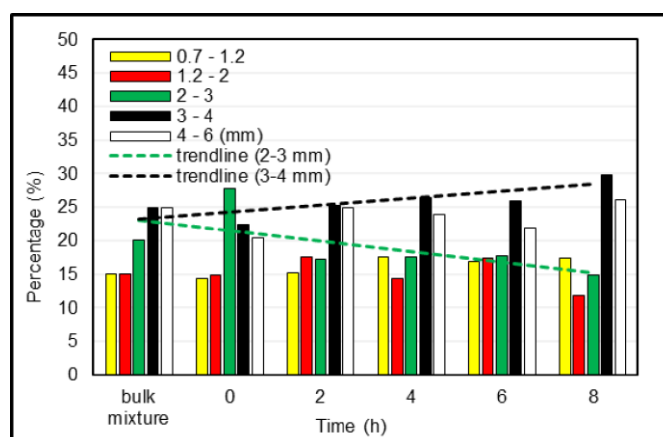
**Figure 3.** Bed and water surface evolution for the reference case, legend: WSL = water surface level, BSL = bed surface level, t = experimental time.

Although the total fed sediment load was equal or very similar to the entrained sediment load for each test run the bed and water surface slopes varied in time even in the simple case of a straight channel.



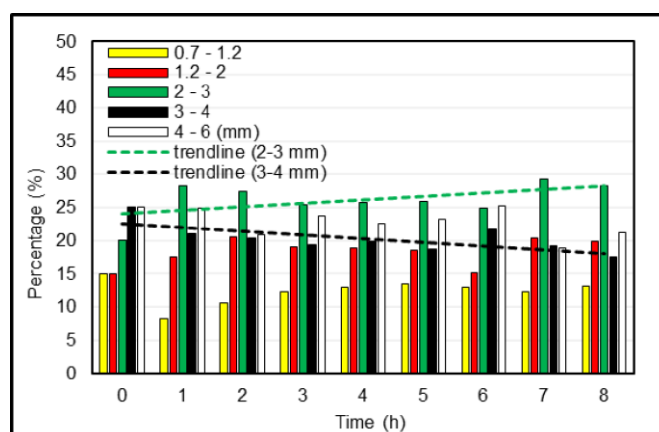
These results were based on the observed process that sediments were transported in bed forms which were typically not covering the whole channel width. Moreover, interestingly the thalweg of the experimental channel changed from one test run to the other. Within a test run the thalweg sometimes changed its course from left in the upstream section to right in the downstream section (or vice versa). Even after eight hours of experiments the dynamic equilibrium slope could not be specified exactly. However, the original assumption that the transported sediment rate corresponds to a bed slope of 0.005 turned out to be quite accurate considering the mean bed and water surface slopes after eight hours of 0.0049 and 0.0048, respectively.

Figure 4 illustrates the grain size distribution of the bed surface after 0, 2, 4, 6 and 8 hours as compared to the bulk grain size distribution of the sediment mixture. The grain size distribution of the bed surface was determined from image processing as described in section 2.4. From the linear trend line for the green sediment fraction (2-3 mm) it becomes obvious that this fraction had the tendency to be washed out of the bed. In contrast the black sediment fraction (3-4 mm) tended to accumulate on the bed surface, thus a coarsening of the experimental bed surface was observed.



**Figure 4.** Grain size distributions of the bed surface from image processing after 0, 2, 4, 6 and 8 hours for the reference case; linear trends for the green and black grain fractions.

The grain size distributions of the entrained sediments after 0, 1, 2, 3, 4, 5, 6, 7 and 8 hours of the reference case are depicted in Figure 5. The grain size distributions were obtained from sieve analyses. A reverse trend as for the bed surface composition (Figure 4) can be observed. The percentage of the green sediments increased while the black fraction decreased in time compared to the bulk distribution. This is not only an interesting result in itself. It also indicates that the two methods for determining the grain size distribution yield consistent results.



**Figure 5.** Grain size distributions of the entrained sediments from sieve analysis after 0, 1, 2, 3, 4, 5, 6, 7 and 8 hours for the reference case; linear trends for the green and black grain fractions.

### 3.2 Delta formation test runs

The delta formation test runs were carried out starting from the final bed levels of the reference case test runs. The discharge was set to  $Q = 0.7 \times Q_{1\text{-year}}$ .

For this discharge all grain fractions were transported in undisturbed normal flow conditions. However, the backwater conditions have a huge effect on the sediment transport capacity. Almost all fed sediments accumulated and remained in the experimental section, i.e. in the vicinity of the head of the reservoir. On average only 3% of the fed sediments were entrained from the experimental section and these sediments consisted of the sand fractions (yellow and red) only. In Table 5 the mean bed and water surface slopes as well as the ratio of fed vs entrained sediment load are summarized.

**Table 5.** Mean bed and water surface slopes and ratio of fed vs entrained sediment load for the delta formation case

Test hour (h)	Bed slope	Water surface slope	Ratio of fed vs entrained sediment load
0	0.0035	0.0044	-
2	0.0034	0.0026	27
4	0.0032	0.0032	36
6	0.0034	0.0027	32
8	0.0044	0.0034	39
mean	0.0036	0.0033	33

In Figure 6 the delta evolution is illustrated after 2, 4, 6 and 8 hours. With each test run the height of the delta raised. The longitudinal extent of the delta propagated in both upstream and downstream direction. The delta formation was accompanied by a rise of the water levels demonstrating the fact that this might cause flood safety issues. During eight hours of experimental time which corresponds to approximately 36 hours at 1:1 scale the bed and water levels raised by 0.49 m and 0.48 m at 1:1 scale, respectively. According to Julien (2010, p.319f) the topset slope of the delta has about half the slope of the original bed. The experimental results yield mean slopes of 0.0049 and 0.0036 for the original bed slope and the delta topset slope, respectively (Table 4 and Table 5). Though the measured topset slope is steeper than predicted by Julien's rule of thumb the experimental result is well in the range of other experimental results and field studies (Julien, 2010, p.319).

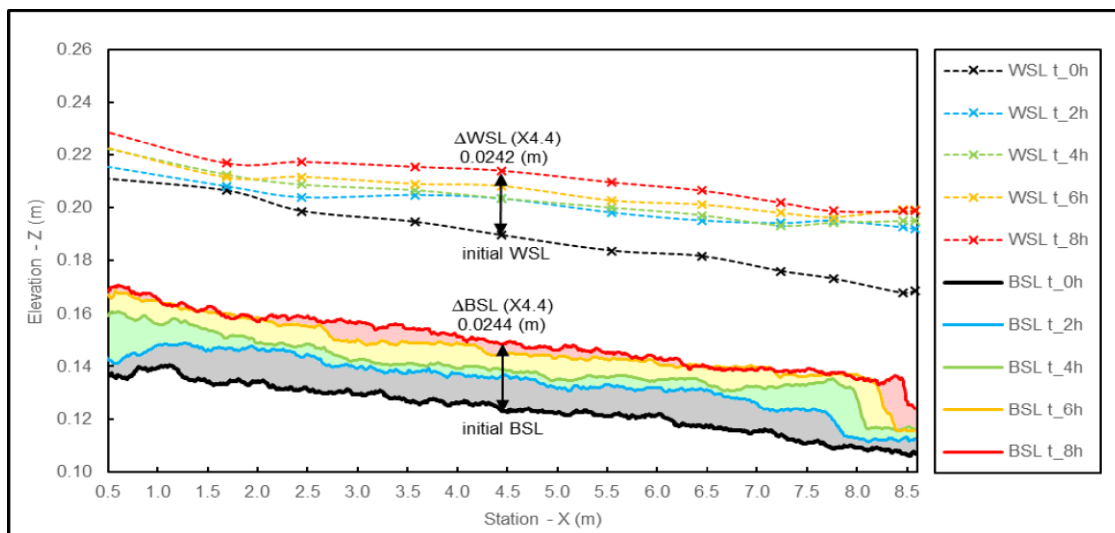


**Figure 6.** Delta evolution after 2, 4, 6 and 8 hours, legend: WSL = water surface level, BSL = bed surface level, t = experimental time.

#### 4 CONCLUSIONS

In this paper experiments on delta formation at the head of a RoR hydro power plant were carried out in a scaled physical model. The model scale was 1:20. The aim of the paper was to study delta formation in a representative medium-sized gravel bed river.

The hydrological and sedimentological conditions were chosen to resemble the Mürz river in Styria, Austria. The delta formation was studied at a discharge of  $Q = 0.7 \times Q_{1\text{-year}}$ . At this flow rate all fractions of the

used sediment mixture were transported. Assuming that this flow rate is too low to evoke a reservoir drawdown it seemed to be a good choice to study delta formation.

A sediment mixture of five different fractions was used covering a range of 14 – 120 mm at 1:1 scale. Each sediment fraction had a different color. A novel image processing method was employed to determine the grain size distribution of the bed surface from images. In addition to this method the fed and entrained sediments were sieved. Prior to the delta formation test runs reference experiments were carried out in a straight river section at an initial slope of 0.005 and at a pre-calculated sediment feeding rate. The reference experiments demonstrated that even under normal flow conditions in a straight channel the bed levels and the thalweg are changing constantly. The mean bed slope was found to be 0.0049. The delta formation experiments revealed that almost all sediments which were easily transported under normal flow conditions accumulated at the head of the reservoir and were not transported further except of a very small percentage of the sand fractions. The delta height increased and the water levels rose considerably underlying the threatening of flooding due to delta formation. The delta propagated both upstream and downstream. As a next step sorting effects within the delta which were clearly visible during the experiments will be analyzed. This investigation forms part of a larger study on reservoir siltation and desiltation in medium-sized gravel bed rivers.

## ACKNOWLEDGEMENTS

The financial support by the Austrian Federal Ministry for Digital and Economic Affairs; the National Foundation of Research, Technology and Development of Austria is gratefully acknowledged. We gratefully acknowledge financial support from the Christian Doppler Research Association.

## REFERENCES

- Annandale, G. W., Randle, T. J., Langendoen, E. J., & Hotchkiss, R. H. (2018). Reservoir sedimentation management: a sustainable development challenge. In A. Findikakis & K. Kadi Abderrezzak (Eds.), *hydrolink 3/2018* (Vol. 3).
- Best, J. (2019). Anthropogenic stresses on the world's big rivers. *Nature Geoscience*, 12(1), 7–21. <https://doi.org/10.1038/s41561-018-0262-x>
- Grill, G., Lehner, B., Thieme, M., Geenen, B., Tickner, D., Antonelli, F., ... Zarfl, C. (2019). Mapping the world's free-flowing rivers. *Nature*, 569(7755), 215–221. <https://doi.org/10.1038/s41586-019-1111-9>
- Habersack, H., Tritthart, M., Liedermann, M., & Hauer, C. (2014). Efficiency and uncertainties in micro- and mesoscale habitat modelling in large rivers. *Hydrobiologia*, 729(1), 33–48. <https://doi.org/10.1007/s10750-012-1429-x>
- Habersack, Helmut, Haspel, D., & Campbell, I. (2013). Integrated management of large river systems. *International Journal of River Basin Management*, 11(2), 137. <https://doi.org/10.1080/15715124.2013.824148>
- Hauer, C. (2015). Review of hydro-morphological management criteria on a river basin scale for preservation and restoration of freshwater pearl mussel habitats. *Limnologia*, 50, 40–53. <https://doi.org/10.1016/j.limno.2014.11.002>
- Hauer, C., Wagner, B., Aigner, J., Holzapfel, P., Flödl, P., Liedermann, M., ... Habersack, H. (2018). State of the art, shortcomings and future challenges for a sustainable sediment management in hydropower: A review. *Renewable and Sustainable Energy Reviews*, 98, 40–55. <https://doi.org/10.1016/j.rser.2018.08.031>
- Julien, P. Y. (2010). *Erosion and Sedimentation* (2nd ed.). New York: Cambridge University Press.
- Sindelar, C., Schobesberger, J., & Habersack, H. (2017). Effects of weir height and reservoir widening on sediment continuity at run-of-river hydropower plants in gravel bed rivers. *Geomorphology*, 291. <https://doi.org/10.1016/j.geomorph.2016.07.007>
- Sindelar, Christine, Tritthart, M., Habersack, H., Pfemeter, M., Sattler, S., & Hengl, M. (2019). Sohlenstabilisierung bei Aufweitungen und geschiebedefizitären Flüssen. *WASSERWIRTSCHAFT*, 109(1), 12–18. <https://doi.org/10.1007/s35147-018-0280-z>
- Wagner, B., Hauer, C., Schoder, A., & Habersack, H. (2015). A review of hydropower in Austria: Past, present and future development. *Renewable and Sustainable Energy Reviews*, 50, 304–314. <https://doi.org/10.1016/j.rser.2015.04.169>